A New Method to Bound the Integrity Risk for Residual-Based ARAIM

Correspondence

This article develops a tight integrity risk bound for residual-based (RB) advanced receiver autonomous integrity monitoring (ARAIM). ARAIM measurement models include nominal biases accounting for unknown but bounded errors, and faults of unbounded magnitude. In RB methods, upper bounding the integrity risk requires that one finds the worst-case directions of both the multisatellite fault vector and of the all-in-view nominal bias vector. Previous methods only account for the worst-case fault direction assuming zero nominal bias. To address this issue, in this article, we derive a new bounding method in parity space. The method establishes a direct relationship between mean estimation error and RB test statistic noncentrality parameter, which accounts for both faults and nominal errors. ARAIM performance is evaluated to quantify the improvement provided by the proposed method over previous approaches.

I. INTRODUCTION

Global navigation satellite systems (GNSS) can provide navigation service for safety critical civilian aviation applications. However, satellite signals are vulnerable to faults, including satellite and constellation faults, which are significant threats to safety. GPS receiver autonomous integrity monitoring (RAIM) is currently used as a means of fault detection (FD) and exclusion in enroute phases of flight. Future dual-frequency and multiconstellation GNSS are motivating the development of a new version of RAIM that can achieve significant navigation performance improvements. This new concept is called advanced receiver autonomous integrity monitoring (ARAIM). ARAIM is expected to meet stringent requirements, for both en-route and final approach, including RNP0.1 ("RNP" stands for required navigation performance) and LPV-200 (localizer precision vertical) [1], [2].

Manuscript received December 29, 2019; revised September 10, 2020; released for publication November 9, 2020. Date of publication November 25, 2020; date of current version April 10, 2021.

DOI. No. 10.1109/TAES.2020.3040527

Refereeing of this contribution was handled by A. Halder.

This work was supported by the National Aeronautics and Space Administration (NASA); Award no. NNX17AJ86A.

Authors' addresses: Peng Zhao is with the School for Engineering of Matter, Transport & Energy, Arizona State University Tempe, AZ 85281 USA, Email: (pzhao28@asu.edu); Mathieu Joerger is with the Kevin T. Crofton Department of Aerospace and Ocean Engineering, Virginia Tech Blacksburg, VA 24061 USA, Email: (joerger@vt.edu); Xiao Liang is with the Telecommunications Team, Ecole Nationale de l'Aviation Civile (ENAC), Toulouse 31400, France, Email: (xiao.liang@enac.fr); Boris Pervan is with the Mechanical Materials and Aerospace Engineering Department at Armour College of Engineering Chicago, IL 60616 USA, Email: (pervan@iit.edu); Yongming Liu is with the School for Engineering of Matter, Transport & Energy, Arizona State University, Tempe, AZ 85281 USA, E-mail: (yongming.liu@asu.edu). (Corresponding author: Yongming Liu.)

0018-9251 © 2020 IEEE

Thus, the measurement error models used in ARAIM are under higher scrutiny than in conventional RAIM. In conventional RAIM, satellite ranging errors are over-bounded by zero-mean Gaussian functions (over-bounded in the CDF sense as described in [3]), whereas ARAIM assumes measurements with nonzero mean, because, for example, of signal deformation and antenna biases. Nominal biases were observed from high-resolution, low-noise measurements in [4]. These biases may be constant or repeatable, but would be cumbersome to calibrate for each individual receiver [5]. Under fault-free conditions, the mean ranging error is modeled as never exceeding a predefined "nominal bias" parameter (the maximum and minimum values of the nominal bias for integrity purposes are $b_{\rm nom} = \pm 0.75 {\rm m}$ [6], [7]).

Two main implementations of ARAIM have been widely used [8]. First, solution separation (SS) [9] is a position domain method that performs FD and exclusion by monitoring the consistency of satellite subset solutions with the all-in-view position. This approach was proposed to solve the integrity problem under multiple fault hypothesis in [10]. Much work has gone into applying this method to ARAIM [6], [11]-[15]. The SS method is used in the ARAIM baseline algorithm for its ability to efficiently deal with multiple simultaneous measurement faults and with nominal biases. A SS ARAIM integrity risk bound accounting for multisatellite unbounded faults and all-in-view bounded biases is derived in [7]. The second approach is chi-squared residual based (RB) RAIM, or equivalently parity-based RAIM [16], [17]. It is a range domain method that detects and excludes faults by comparing observed versus estimated pseudoranges [18]. RB RAIM is often implemented using a least-square estimator. Assuming that nominal ranging error vector follows a known multivariate Gaussian distribution, the sum of squares of the residuals weighted by the inverse measurement error covariance matrix is the RB detection test statistic. It follows a chi-square distribution under fault-free conditions, and a noncentral chi-square distribution under faulted conditions. The RB method has mostly been implemented to account for single-satellite faults assuming zero-mean Gaussian range errors [17], [19]. Reference [20] identifies the differences between the SS and RB methods. An analytical expression of the worst-case fault, which maximizes the integrity risk assuming zero nominal bias, is given in [8] and [21].

Although the baseline ARAIM algorithm is derived using SS, receiver manufacturers who previously used RB approaches in their GPS-based RAIM products may prefer implementing RB methods in multiconstellation ARAIM to ensure compatibility with legacy products. But there is currently no RB ARAIM method designed to efficiently account for both multisatellite unbounded faults and all-inview bounded biases. Thus, it is unclear whether or not RB ARAIM can provide tighter integrity risk bounds than SS ARAIM. The objective of this article is to address this gap.

In this article, we derive a new RB method that tightly bounds the integrity risk by directly expressing the mean positioning error in terms of the noncentrality parameter of the noncentrally chi-square distributed RB detection test statistic. This expression not only accounts for unbounded faults affecting a subset of measurements as in [8], [17], [19]–[23], but also accounts for nominal, bounded biases simultaneously affecting all measurements. A performance analysis illustrates the fact that a tight integrity risk bound is achieved.

II. RELATED WORK

A. Position Estimation Error

Let *n* be the number of visible satellites. The measurement equation can be expressed as follows:

$$z = Hx + b + v + f \tag{1}$$

where z is a $n \times 1$ vector of range measurements from user to satellite, normalized following the process described in [8], H is an $n \times m$ normalized observation matrix, m is the number of state parameters to be estimated, x is the $m \times 1$ position and receiver clock parameter vector, b is the $n \times 1$ normalized nominal bias vector, f is the f is the f in a normalized fault vector, and f is the f in a normalized measurement noise vector composed of zero-mean, unit-variance independent, and identically distributed (i.i.d.) random variables. The nominal bias is an unknown error having lower and upper bounds (the maximum and minimum values of this nominal bias for integrity purposes are f in f in

The least-squares estimate of x is expressed as follows:

$$\hat{\boldsymbol{x}}_0 = \boldsymbol{H}^* \boldsymbol{z} \tag{2}$$

where subscript 0 indicates the all-in-view solution, using all available measurements. H^* is the left pseudoinverse of H, and is defined as

$$\boldsymbol{H}^* = (\boldsymbol{H}^T \boldsymbol{H})^{-1} \boldsymbol{H}^T \tag{3}$$

Substituting (1) into (2), we have

$$\hat{\mathbf{x}}_0 = \mathbf{H}^* \mathbf{z} = \mathbf{H}^* \left(\mathbf{H} \mathbf{x} + \mathbf{b} + \mathbf{v} + f \right) = \mathbf{x} + \mathbf{H}^* \left(\mathbf{b} + \mathbf{v} + f \right). \tag{4}$$

The positioning error for the state of interest, resulting from the difference between the state estimate and the true state, is expressed as follows:

$$\varepsilon_0 = e_d^T \left(\hat{x} - x \right) = h^{*T} \left(v + b + f \right)$$
 (5)

where e_d is a $m \times 1$ column vector used to extract the state of interest in x, for example, using $e_d = [0 \ 0 \ 1 \ 0]^T$ to extract the vertical position state (assuming a single constellation, i.e., a single receiver clock bias parameter), h^* is a $n \times 1$ column vector made of the row of H^* corresponding to the state of interest ($h^* = [e_d^T H^*]^T$). The term $h^{*T}b$ on the right-hand side of (5) captures the impact of nominal bias on the state estimate error. Since v is composed of zeromean, unit-variance i.i.d. Gaussian variables, ε_0 follows a Gaussian distribution whose mean value is

$$E\left(\varepsilon_{0}\right) = \boldsymbol{h}^{*T}\left(\boldsymbol{b} + \boldsymbol{f}\right). \tag{6}$$

B. RB ARAIM FD Method

To mitigate the impact of a fault vector f simultaneously impacting a number of satellites n_i , we can use self-contained (or, receiver autonomous) redundancy-based methods if the number of visible satellites n is larger than or equal to $m + n_i$. The case where $n < m + n_i$ impacts continuity and is beyond the scope of this article. Parity-based detection methods are equivalent to RB approaches. The $(n - m) \times n$ parity matrix Q is defined such that its rows form an orthonormal basis for the left null space of the measurement matrix H, i.e.,

$$QH = 0 \tag{7}$$

$$QQ^T = I_{n-m} \tag{8}$$

$$Q^T Q = S \tag{9}$$

where I_n is an $n \times n$ identity matrix. An equivalent expression of the $n \times n$ matrix S is given by: $S = I_n - HH^*$. The row space of Q is the parity space of H [22]. Projected in parity space, the measurement vector z, fault vector f, measurement noise vector v and nominal bias vector v become v become v and v become v become

Vector p is the parity vector, which can be expressed as follows:

$$p = Qz = Q(Hx + b + v + f) = p_b + p_v + p_f$$
 (10)

Because v is composed of zero-mean, unit-variance i.i.d. random variables, elements of p_v follow a Gaussian distribution. The covariance matrix of these elements is written as follows:

$$\operatorname{cov}(p_{v}, p_{v}) = \operatorname{cov}(Qv, Qv) = Q\operatorname{cov}(v, v)Q^{T} = I_{n-m}$$
(11)

which indicates that the elements of p_v are zero-mean, unit-variance i.i.d. random variables. Therefore, we can express the parity-based (or equivalently, the RB) detection test statistic as

$$q = \|\mathbf{p}\|_{2}^{2} \sim \chi^{2} (n - m, \lambda^{2})$$
 (12)

where we used the notation $\|\boldsymbol{p}\|_2^2 = \boldsymbol{p}^T \boldsymbol{p}$, and $\chi^2(n-m, \lambda^2)$ designate a noncentral chi-square distribution with k degrees of freedom and noncentrality parameter, or NCP, λ^2 . In this case, λ^2 is expressed as follows:

$$\lambda^2 = \| \boldsymbol{p}_f + \boldsymbol{p}_h \|_2^2. \tag{13}$$

If q exceeds a threshold T_{χ^2} , a fault has been detected. The detection threshold is given by the following:

$$T_{\chi^2} = \chi_{n-m \lambda_0}^{-2} \left(P_{fa} \right) \tag{14}$$

where P_{fa} is the required probability for false alarm, and $\lambda_0^2 = \mathbf{p}_b^T \mathbf{p}_b$ [21]. This threshold ensures the continuity of ARAIM operation that may interrupt by false alarm.

C. Integrity Risk Evaluation

ARAIM performs autonomous FD and integrity monitoring in the airborne receiver. Integrity monitoring is defined as the timely provision of information to users about the level of trustworthiness of the navigation system

[23]–[25]. The integrity risk or probability of hazardous misleading information (HMI) is the risk of the positioning error exceeding the alert limit while the detection test statistic is below the threshold. The probability of HMI is expressed as follows:

$$P_{\rm HMI} = P\left({\rm HI}, \bar{D}\right) \tag{15}$$

where hazardous information HI is the event of the positioning error exceeding the alert limit, and \bar{D} is the no-detection event, which indicates the test statistic is lower than the threshold. To bound the integrity risk, we consider all possible fault hypotheses. The integrity risk can be expressed as [7] follows:

$$P_{\text{HMI}} \le \sum_{i=0}^{h} P\left(\left|\varepsilon_{0}\right| > l, q\left\langle T_{\chi^{2}}\right| H_{i}\right) P\left(H_{i}\right) \tag{16}$$

where ε_0 is the error of position estimation, l is the alert limit (i.e., a predefined limit on acceptable errors, e.g., specified in [2] for ARAIM), T_{χ^2} is the threshold for test statistic q, h is the total number of fault hypotheses, H_i is the ith hypothesis, and i=0 is the fault-free hypothesis index. Because the RB test statistic and the least-squares positioning error are statistically independent [8], [14], the inequality in (16) can be rewritten as follows:

$$P_{\text{HMI}} \le \sum_{i=0}^{h} P(|\varepsilon_0| > l|H_i) P(q\langle T_{\chi^2} | H_i) P(H_i)$$
 (17)

which facilitates the calculation of the integrity risk bound.

III. PROPOSED INTEGRITY RISK BOUNDING METHOD

In previous RB implementations [8], [17], [19]–[21], [23], the integrity risk bound was evaluated by: first, upper-bounding the failure mode slope (FMS), i.e., the ratio of mean estimation error over test statistic's NCP, which is equivalent to finding the worst-case fault vector direction [21]; and then, determining the maximum probability of HMI over all possible fault magnitudes using a one-dimensional search process. In contrast, in this section, we focus on upper-bounding the mean estimation error, but we directly express it in terms of the test statistic's NCP. This provides the means to not only account for faults impacting a sunset of measurements, but also for nominal bounded errors potentially affecting all observations.

A. Upper Bound on Positioning Error

The error of the least square position estimation follows a Gaussian distribution [8], with standard deviation σ_0 . Under the fault-free hypothesis (for i = 0), the mean value of estimation error is obtained using (6), and is given by the following:

$$E\left(\varepsilon_{0}\right) = \boldsymbol{h}^{*T}\boldsymbol{b} \tag{18}$$

Therefore, the absolute value of the positioning error can be bounded using the following inequality:

$$|E(\varepsilon_0)| \le |\mathbf{h}^{*T}| \cdot 1_{n \times 1} \times b_{\text{nom}} \text{ under } H_i \text{ for } i = 0$$
 (19)

where $|\cdot|$ designates the element-wise absolute value of the vector argument, $1_{n\times 1}$ is an $n\times 1$ vector of ones, b_{nom} is the maximum value of the nominal bias.

Under the ith ($i \neq 0$) fault hypothesis, let n_i be the number of faulty measurements in the ith subset for $i = 1, \ldots, h$. To facilitate exposition, we assume without loss of generality that the ith subset corresponds to the first n_i elements of z. Note that n_i is no greater than n-m, otherwise the fault may be undetectable [8]. In ARAIM and in other GNSS-based applications, the prior probability of faults impacting more than n-m measurements is small enough that it can be budgeted out of the integrity risk requirement [2], [6]–[8]. The mean value of the all-in-view positioning error $|E(\varepsilon_0)|$ is bounded using the following inequality:

$$|E\left(\varepsilon_{0}\right)| \leq \bar{g}_{i} \left| \boldsymbol{w}_{i}^{T} \left(\boldsymbol{p}_{f} + \boldsymbol{p}_{b}\right) \right| + c_{i} \text{ for } i = 1, \dots, h \quad (20)$$

where

$$\boldsymbol{w}_{i}^{T} = \frac{1}{\bar{\varrho}_{i}} \boldsymbol{h}^{*} \boldsymbol{A}_{i} (\boldsymbol{A}_{i}^{T} \mathbf{S} \boldsymbol{A}_{i})^{-1} \boldsymbol{A}_{i}^{T} \boldsymbol{Q}^{T}$$
(21)

$$c_i = \left| \boldsymbol{h}_i^{*T} \right| \cdot \mathbf{1}_{n \times 1} \times b_{\text{nom}} \tag{22}$$

$$\bar{g}_i = \sqrt{\boldsymbol{h}^* \boldsymbol{A}_i (\boldsymbol{A}_i^T \mathbf{S} \boldsymbol{A}_i)^{-1} \boldsymbol{A}_i^T \boldsymbol{h}^{*T}} \text{ for } i = 1, \dots, h.$$
 (23)

 \mathbf{w}_{i}^{T} is a unit vector after normalization by $\bar{\mathbf{g}}_{i}$, \mathbf{h}^{*} is the row of \mathbf{H}^{*} corresponding to the state of interest, $A_{i} = [\mathbf{I}_{n_{i}}, 0_{n_{i} \times (n-n_{i})}]^{T}$ is a $n \times n_{i}$ matrix with $\mathbf{I}_{n_{i}}$ occupying the first $n_{i} \times n_{i}$ block and with zeros occupying the other block, \mathbf{h}_{i}^{*} is the row of \mathbf{H}_{i}^{*} corresponding to the state of interest and \mathbf{H}_{i}^{*} is obtained using (3) by setting the ith row of \mathbf{H} to zero. Appendix gives a proof of (20).

Because \mathbf{w}_i^T is unit magnitude, by substituting λ for $\|\mathbf{p}_f + \mathbf{p}_b\|_2$ as defined in (13), we can further bound the positioning error in (20) using the following inequality:

$$|E\left(\varepsilon_{0}\right)| \leq \bar{g}_{i} \left| \boldsymbol{w}_{i}^{T} \left(\boldsymbol{p}_{f} + \boldsymbol{p}_{b} \right) \right| + c_{i} \leq \bar{g}_{i} \|\boldsymbol{p}_{f} + \boldsymbol{p}_{b}\|_{2} + c_{i}$$

$$= \bar{g}_{i} \lambda + c_{i} \text{ for } i = 1, \dots, h. \tag{24}$$

This positioning error bound has a linear relationship with the square root of the detection test statistic's NCP λ .

It is worth noting that \bar{g}_i in (23) is equal to the worst-case FMS in [8] and [21]. However, the method in [8] and [21] only accounted for zero mean measurement errors on a subset of measurements. Equation (24) allows for all measurements to be impacted by nominal biases, and for a subset of measurements to be faulty, while still guaranteeing a bound on $E(\varepsilon_0)$.

For consistency of notations between fault-free and fault hypotheses, we extend the definition of \bar{g}_i ($i \neq 0$) in (23) to include the fault-free hypothesis (i = 0) with $\bar{g}_0 = 0$:

$$\bar{g}_i = \begin{cases} 0 \text{ if } i = 0\\ \sqrt{\boldsymbol{h}^* A_i (\boldsymbol{A}_i^T \mathbf{S} \boldsymbol{A}_i)^{-1} \boldsymbol{A}_i^T \boldsymbol{h}^{*T}} \text{ if } i \neq 0 \end{cases}$$
 (25)

where i=0 indicates the fault-free hypothesis. Other notations remain unchanged. For example, by definition of \boldsymbol{h}_i^* , we use the notation $\boldsymbol{h}^* = \boldsymbol{h}_0^*$, and c_0 is $c_0 = |\boldsymbol{h}^{*T}| \cdot 1_{n \times 1} \times b_{\text{nom}}$ in (19). Vector \boldsymbol{w}_i^T in (21), where the inverse of \bar{g}_i is taken, is no longer needed. Therefore, the positioning error

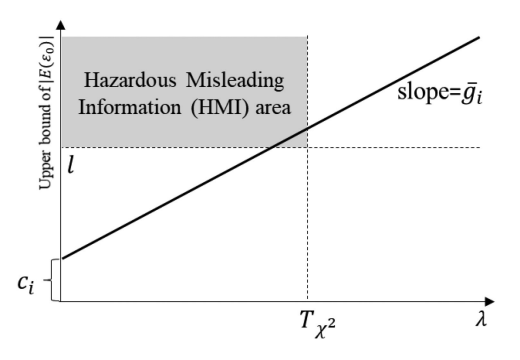


Fig. 1. Illustration of HMI probability bounding method. The square root of the non-centrality parameter λ and upper bound of $|E(\varepsilon_0)|$ are related by the slope \overline{g}_i . The probability of HMI (P_{HMI}) is upper-bounded by searching over values of λ till a maximum in P_{HMI} is found.

bound is given by the following:

$$|E(\varepsilon_0)| \le \bar{g}_i \lambda + c_i \text{for } i = 0, \dots, h$$
 (26)

B. Integrity Risk Evaluation

As expressed in (17), the RB integrity risk can be expressed as the sum over all fault-free and fault hypotheses of the product of the probability of hazardous information $P(|\varepsilon_0| > l|H_i)$ and the risk of no detection $P(q\langle T_{\chi^2}|H_i)$ weighted by $P(H_i)$.

When evaluating the $P_{\rm HMI}$ contribution under the fault-free hypothesis, (25) and (26) are used to obtain an upper-bound on $P(|\varepsilon_0| > l|H_0)$. In addition, an upper bound on $P(q\langle T_{\chi^2}|H_0)$ is obtained considering the fact that λ is lower bounded by 0.

Under a fault hypothesis, fault and bias both impact $|\varepsilon_0|$ and q. We have expressed $|\varepsilon_0|$ and q in terms of λ . In particular, using (26), we can upper-bound the mean positioning error for any value of λ . Thus, a one-dimensional search over λ -values can be performed to determine the maximum $P_{\rm HMI}$ in (17), as illustrated in Fig. 1. This section has proved that an upper-bound on $P_{\rm HMI}$ can be regarded as considering the worst-case fault mode slope (as in [21]), and shifting the failure mode line up by c_i to account for nominal measurement errors.

IV. PERFORMANCE ANALYSIS

To demonstrate the reduction in integrity risk brought by the proposed method as compared to prior work on RB ARAIM in [21] and to SS ARAIM [8], [26], two example applications are considered: an illustrative single-state, three-measurement example, which is also used in [21] and [27], and an example of availability performance analysis of ARAIM FD for worldwide vertical guidance of aircraft assuming dual-frequency measurements from baseline GPS and Galileo constellations [7].

A. Illustrative Single-State Three-Measurement Example

For the illustrative single-state, three-measurement example, simulation parameters are given in Table I. This example only considers the single fault hypothesis. The integrity risk is evaluated versus a range of alert limit

TABLE I Simulation Parameters

| NameValueObservation Matrix $\boldsymbol{H} = [1\ 1\ 1]^T$ Noise $\boldsymbol{v} \sim N(\boldsymbol{0}, \boldsymbol{I})$ False Alarm Probability $P_{fa} = 10^{-6}$ Prior Fault Probability $P_{Hi} = 10^{-3}$ Alert Limit $l = 0.5$ to $4m$ Maximum Nominal Bias $b_{nom} = 0.75m$ | | |
|---|-------------------------|---|
| Noise $v \sim N(0, I)$ False Alarm Probability $P_{fa} = 10^{-6}$ Prior Fault Probability $P_{Hi} = 10^{-3}$ Alert Limit $l = 0.5$ to $4m$ | Name | Value |
| False Alarm Probability $P_{fa} = 10^{-6}$ Prior Fault Probability $P_{Hi} = 10^{-3}$ Alert Limit $l = 0.5$ to $4m$ | Observation Matrix | $\boldsymbol{H} = [1 \ 1 \ 1]^T$ |
| Prior Fault Probability $P_{Hi} = 10^{-3}$ Alert Limit $l = 0.5$ to $4m$ | Noise | $\boldsymbol{v} \sim N(\boldsymbol{0}, \boldsymbol{I})$ |
| Alert Limit $l = 0.5 \text{ to } 4m$ | False Alarm Probability | $P_{fa} = 10^{-6}$ |
| | Prior Fault Probability | $P_{Hi} = 10^{-3}$ |
| Maximum Nominal Bias $b_{nom} = 0.75m$ | Alert Limit | l = 0.5 to $4m$ |
| | Maximum Nominal Bias | $b_{nom} = 0.75m$ |

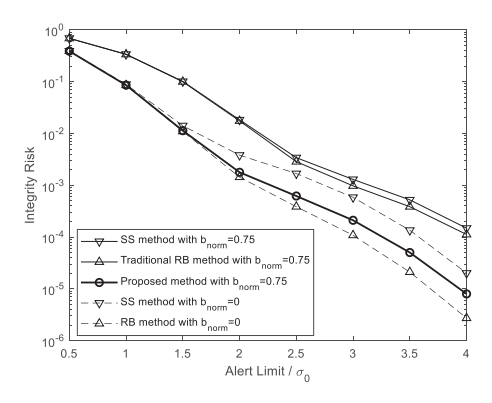


Fig. 2. Comparison of integrity risk values using different ARAIM methods, and different nominal bias bounding methods. The figure shows the sensitivity of the integrity risk versus alert limit (normalized by state estimate error standard deviation) on the *X*-axis.

values, for conventional RB and SS ARAIM methods. Two values of the nominal bias are considered: $b_{\text{nom}} = 0\text{m}$, and $b_{\text{nom}} = 0.75\text{m}$, in which case the proposed method becomes relevant in comparison to SS and the previous RB ARAIM method in [21].

For this illustrative example, Fig. 2 presents values of the integrity risk for a range of alert limits (normalized by the state estimation error standard deviation). For $b_{\rm nom}=0$ m, the differences between the RB and SS ARAIM approaches are analyzed in detail in [8]. For $b_{\rm nom}=0.75$ m, the proposed RB ARAIM method outperforms both SS ARAIM and the RB ARAIM approach given in [21]. For the entire range of alert limits under consideration, the new method's integrity risk bound is almost an order of magnitude lower than previous SS and RB ARAIM approaches. The new bound assuming $b_{\rm nom}=0.75$ m approaches that of conventional methods that assume $b_{\rm nom}=0$ m.

Worldwide Availability Performance of the Proposed Method

In this section, we evaluate the availability performance of ARAIM FD algorithm for worldwide vertical guidance of aircraft assuming dual-frequency measurements from baseline GPS and Galileo constellations. LPV-200 availability maps are shown in Figs. 3 and 4, which, respectively, present the availability of the SS method and of the proposed RB method. Availability is computed for a 10 deg-by-10 deg grid of locations, and is color-coded from red to blue corresponding to values of 95–100%. Coverage performance

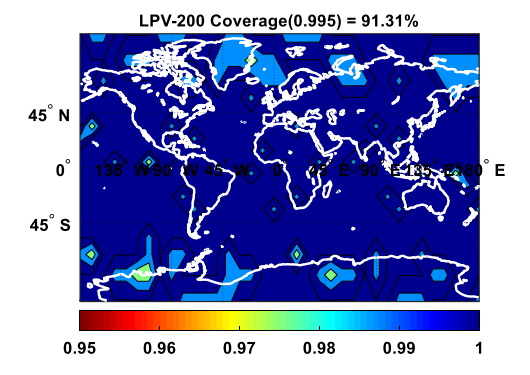


Fig. 3. Worldwide LPV-200 availability performance of SS-ARAIM FD algorithm. This performance evaluation employs an optimized estimator proposed in [12].

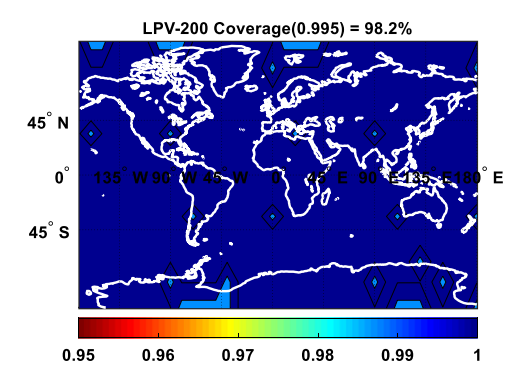


Fig. 4. Worldwide LPV-200 availability performance of the proposed algorithm.

TABLE II Simulation Parameters

| Name | Value |
|--|----------------------|
| Integrity Risk Requirement | 10 ⁻⁷ |
| Alert Limit Requirement | 35m |
| Continuity Budget Allocated to The | 1.3×10^{-6} |
| Vertical Mode | |
| Prior Probability of Satellite Fault | 10 ⁻⁵ |
| Prior Probability of Constellation Fault | 10-4 |
| URA/URE | 1.5m/1m |
| Nominal Bias | 0.75m |
| | |

is given in the figures' titles: coverage is defined as the percentage of locations that meet an availability performance greater than 99.5%. This percentage is weighted by the cosine of the location's latitude because low latitude regions represent larger surfaces. For short, this metric is noted coverage of >99.5% availability, or simply coverage. The conventional RB method is not evaluated because the conventional RB method cannot account for both multisatellite unbounded faults and all-in-view bounded biases. The main parameters for this simulation are listed in Table II.

Fig. 3 illustrates the worldwide LPV-200 availability performance using SS-ARAIM algorithm. In the simulation, an optimized estimator proposed in [12] is employed to improve the performance. The result indicates that >99.5%

coverage, i.e., the percentage of locations that achieve better than 99.5% availability, using SS method is 91.31%. The result of the proposed method in this paper is shown in Fig. 4, which demonstrates 98.2% of the world locations achieve availability better than 99.5%. This result indicates that the proposed method outperforms the SS-ARAIM.

V. CONCLUSION

This article describes a new approach to bound the impact of nominal measurement biases on integrity risk in RB ARAIM. A method is derived to find a tight bound on the integrity risk when using an RB test statistic for FD. The proposed method was evaluated using illustrative examples, as well as in more realistic ARAIM LPV-200 availability coverage example. Under the configuration described in this article, the proposed method achieved navigation service coverage improvement as compared to SS ARAIM.

APPENDIX

For this proof, we consider a fault-free subset solution. Subset solutions are used in the derivation, but are not needed in practical implementation. In order to formulate the position estimate calculated by the fault-free satellite subset, we set to zero the row (or rows) corresponding to the *i*th fault hypothesis. The observation matrix becomes

$$\boldsymbol{H}_{i} = \left(\boldsymbol{I} - \boldsymbol{A}_{i} \boldsymbol{A}_{i}^{T}\right) \boldsymbol{H} \tag{27}$$

where $A_i = [I_{n_i}, \mathbf{0}_{n_i \times (n-n_i)}]^T$ is the number of faults, A_i is $n \times n_i$ with I_{n_i} occupying the first n_i rows and columns, otherwise zero. Here, without losing generality, it is assumed that the hypothetical faulty measurements are the first n_i elements of z. Then, the solution of the fault-free subset can be written as follows:

$$\hat{\boldsymbol{x}}_i = (\boldsymbol{H}_i^T \boldsymbol{H}_i)^{-1} \boldsymbol{H}_i^T \boldsymbol{z} = \boldsymbol{H}_i^* \boldsymbol{z}. \tag{28}$$

Thus, the \hat{x}_i is not affected by the fault. Then, we have

$$E(\hat{x}_i) = H_i^* z = H_i^* (H_i x + b + f_i) = x + H_i^* b.$$
 (29)

where x is the true state

We consider the term $H_i^T H_i$ that can be expressed as follows:

$$H_i^T H_i = H^T \left(I - A_i A_i^T \right) H = H^T H - H^T A_i \left(H^T A_i \right)^T.$$
(30)

According to Woodbury's Formula, the inverse matrix is deduced as follows:

$$(\boldsymbol{H}_{i}^{T}\boldsymbol{H}_{i})^{-1} = (\boldsymbol{H}^{T}\boldsymbol{H})^{-1} - \boldsymbol{H}^{*}\boldsymbol{A}_{i} \left(-\boldsymbol{I} + (\boldsymbol{H}^{T}\boldsymbol{A}_{i})^{T}\boldsymbol{H}^{*}\boldsymbol{A}_{i}\right)^{-1} \times (\boldsymbol{H}^{T}\boldsymbol{A}_{i})^{T}(\boldsymbol{H}^{T}\boldsymbol{H})^{-1}$$

$$= (\boldsymbol{H}^{T}\boldsymbol{H})^{-1} + \boldsymbol{H}^{*}\boldsymbol{A}_{i}(\boldsymbol{A}_{i}^{T}\boldsymbol{S}\boldsymbol{A}_{i})^{-1}\boldsymbol{A}_{i}^{T}\boldsymbol{H}^{*T}. (31)$$

We rewrite H_i^* as follows:

$$H_i^* = (H_i^T H_i)^{-1} H_i^T = (H_i^T H_i)^{-1} H^T (I - A_i A_i^T).$$
 (32)

Substituting (31) we have

$$\boldsymbol{H}_{i}^{*} = \left(\left(\boldsymbol{H}^{T} \boldsymbol{H} \right)^{-1} \boldsymbol{H}^{T} + \boldsymbol{H}^{*} \boldsymbol{A}_{i} \left(\boldsymbol{A}_{i}^{T} \boldsymbol{S} \boldsymbol{A}_{i} \right)^{-1} \boldsymbol{A}_{i}^{T} \boldsymbol{H}^{*T} \boldsymbol{H}^{T} \right) \times \left(\boldsymbol{I} - \boldsymbol{A}_{i} \boldsymbol{A}_{i}^{T} \right). \tag{33}$$

Substituting (I - S) for $H^{*T}H^T$, the above equation becomes

$$H_{i}^{*} = \left(H^{*} + H^{*}A_{i}(A_{i}^{T}SA_{i})^{-1}A_{i}^{T} (I - S)\right) \left(I - A_{i}A_{i}^{T}\right)$$

$$= H^{*} - H^{*}A_{i}A_{i}^{T} + H^{*}A_{i}(A_{i}^{T}SA_{i})^{-1}A_{i}^{T}$$

$$- H^{*}A_{i}(A_{i}^{T}SA_{i})^{-1}A_{i}^{T}A_{i}A_{i}^{T}$$

$$- H^{*}A_{i}(A_{i}^{T}SA_{i})^{-1}A_{i}^{T}S + H^{*}A_{i}(A_{i}^{T}SA_{i})^{-1}A_{i}^{T}SA_{i}A_{i}^{T}$$

$$= H^{*} - H^{*}A_{i}A_{i}^{T} + H^{*}A_{i}(A_{i}^{T}SA_{i})^{-1}A_{i}^{T}$$

$$- H^{*}A_{i}(A_{i}^{T}SA_{i})^{-1}A_{i}^{T} - H^{*}A_{i}(A_{i}^{T}SA_{i})^{-1}A_{i}^{T}S$$

$$+ H^{*}A_{i}A_{i}^{T}$$

$$= H^{*} - H^{*}A_{i}(A_{i}^{T}SA_{i})^{-1}A_{i}^{T}S$$
(34)

Thus, we have

$$H^* - H_i^* = H^* A_i (A_i^T S A_i)^{-1} A_i^T S$$
 (35)

To facilitate the derivation of the estimation error in terms of the parity vector, we introduce a notation from SS methods. This is an intermediary step in the derivation. The final expression will be in terms of RB quantities (i.e., of parity vector components). Relationships between SS and RB test statistics are derived in [8]. The difference between \hat{x}_0 and \hat{x}_i (the SS vector) is expressed as follows:

$$\Delta \hat{x} = \hat{x}_0 - \hat{x}_i = (H^* - H_i^*) z = H^* A_i (A_i^T S A_i)^{-1} A_i^T S z.$$
(36)

Substituting the definition of matrix S in (9) into (36), we have

$$\Delta \hat{x} = H^* A_i (A_i^T S A_i)^{-1} A_i^T Q^T Q z = H^* A_i (A_i^T S A_i)^{-1} A_i^T Q^T p.$$
(37)

The mean of $\Delta \hat{x}$ is expressed as

$$E\left(\Delta\hat{x}\right) = H^*A_i \left(A_i^T S A_i\right)^{-1} A_i^T Q^T \left(p_f + p_b\right)$$
(38)

Taking the expectation of the SS $\Delta \hat{x}$ in (36) and substituting into (29), we find the following equation:

$$E(\Delta \hat{x}) = E(\hat{x}_0) - E(\hat{x}_i) = E(\hat{x}_0) - x - H_i^* b$$

= $E(\varepsilon_0) - H_i^* b$ (39)

where ε_0 is the error of the estimate \hat{x}_0 .

The estimate error ε_0 for the state of interest is obtained using the vector \mathbf{e}_d , and is expressed as follows:

$$\varepsilon_0 = \boldsymbol{e_d}^T \ \boldsymbol{\varepsilon}_0 \tag{40}$$

where d = 1, 2, 3 designates three dimensions of position, e.g. east, north, and up, e_d denotes a $m \times 1$ vector whose dth element is 1 and other elements are zeros.

Extracting the state of interest and substituting (38), (39) can be transformed into

$$E(\varepsilon_{0}) = E(\Delta \hat{x}) + \boldsymbol{h}_{i}^{*}\boldsymbol{b}$$

$$= \boldsymbol{h}^{*}\boldsymbol{A}_{i}(\boldsymbol{A}_{i}^{T}\boldsymbol{S}\boldsymbol{A}_{i})^{-1}\boldsymbol{A}_{i}^{T}\boldsymbol{Q}^{T}(\boldsymbol{p}_{f} + \boldsymbol{p}_{b}) + \boldsymbol{h}_{i}^{*}\boldsymbol{b}$$

$$= \tilde{\boldsymbol{w}}_{i}^{T}(\boldsymbol{p}_{f} + \boldsymbol{p}_{b}) + \boldsymbol{h}_{i}^{*}\boldsymbol{b}$$
(41)

where

$$\tilde{\boldsymbol{w}}_{i}^{T} = \boldsymbol{h}^{*} \boldsymbol{A}_{i} (\boldsymbol{A}_{i}^{T} \boldsymbol{S} \boldsymbol{A}_{i})^{-1} \boldsymbol{A}_{i}^{T} \boldsymbol{Q}^{T}$$
(42)

the scalar $\Delta \hat{x}$ is extracted from vector $\Delta \hat{x}$ using

$$\Delta \hat{x} = e_d^T \Delta \hat{x}. \tag{43}$$

 h^* is the row of H^* corresponding to the state of interest $(h^* = e_d^T H^*)$, and h_i^* is the row of H_i^* corresponding to the state of interest $(h_i^* = e_d^T H_i^*)$. The magnitude of \tilde{w}_i^T is calculated as

$$\bar{g}_{i} = \sqrt{\tilde{\boldsymbol{w}}_{i}^{T} \tilde{\boldsymbol{w}}_{i}} \\
= \sqrt{\boldsymbol{h}^{*} A_{i} (\boldsymbol{A}_{i}^{T} \boldsymbol{S} \boldsymbol{A}_{i})^{-1} \boldsymbol{A}_{i}^{T} \boldsymbol{Q}^{T} \boldsymbol{Q} A_{i} (\boldsymbol{A}_{i}^{T} \boldsymbol{S} \boldsymbol{A}_{i})^{-1} \boldsymbol{A}_{i}^{T} \boldsymbol{h}^{*T}} \\
= \sqrt{\boldsymbol{h}^{*} A_{i} (\boldsymbol{A}_{i}^{T} \boldsymbol{S} \boldsymbol{A}_{i})^{-1} \boldsymbol{A}_{i}^{T} \boldsymbol{h}^{*T}}. \tag{44}$$

Then, we normalize $\tilde{\boldsymbol{w}}_{i}^{T}$ as

$$\boldsymbol{w}_{i}^{T} = \frac{1}{\bar{g}_{i}} \boldsymbol{h}^{*} A_{i} (\boldsymbol{A}_{i}^{T} \boldsymbol{S} \boldsymbol{A}_{i})^{-1} \boldsymbol{A}_{i}^{T} \boldsymbol{Q}^{T}. \tag{45}$$

Therefore, Eq. (41) can be rewritten as

$$E\left(\varepsilon_{0}\right) = \bar{\mathbf{g}}_{i} \mathbf{w}_{i}^{T} \left(\mathbf{p}_{f} + \mathbf{p}_{b}\right) + \mathbf{h}_{i}^{*} \mathbf{b}. \tag{46}$$

Using triangle inequality, we have

$$|E\left(\varepsilon_{0}\right)| \leq \bar{g}_{i} \left| \boldsymbol{w}_{i}^{T} \left(\boldsymbol{p}_{f} + \boldsymbol{p}_{b}\right) \right| + \left| \boldsymbol{h}_{i}^{*} \boldsymbol{b} \right| \leq \bar{g}_{i} \left| \boldsymbol{w}_{i}^{T} \left(\boldsymbol{p}_{f} + \boldsymbol{p}_{b}\right) \right| + c_{i}. \tag{47}$$

where $c_i = |\boldsymbol{h}_i^{*T}| \cdot \boldsymbol{1}_{n \times 1} \times b_{\text{nom}}$ is a bound of $|\boldsymbol{h}_i^{*}\boldsymbol{b}|$. Now, (20) has been proved.

ACKNOWLEDGMENT

The work related to this research were performed at the Prognostic Analysis and Reliability Assessment Lab at Arizona State University

PENG ZHAO

Arizona State University, Tempe, AZ, USA

MATHIEU JOERGER ^(D), Senior Member, IEEE Virginia Tech Blacksburg, VA, USA

XIAO LIANG

Ecole Nationale de l'Aviation Civile (ENAC), Toulouse, France

BORIS PERVAN Denior Member, IEEE Armour College of Engineering, Chicago, IL,

YONGMING LIU

Arizona State University, Tempe, AZ, USA

REFERENCES

FAA, G. Panel

Phase II of the GNSS evolutionary architecture study Feb. 2010. [Online]. Available: https://www.faa.gov/about/ office_org/headquarters_offices/ato/service_units/techops/ navservices/gnss/library/documents/media/GEASPhaseII_ Final.pdf

- [2] FAA, "EU-U.S. Cooreration on Satellite Navigation Working Group C - ARAIM Technical Subgroup Milestone 3 Report Feb. 2016.
- J. Rife, S. Pullen, P. Enge, and B. Pervan

Paired Overbounding for nonideal LAAS and WAAS error distributions

IEEE Trans. Aerosp. Electron. Syst., vol. 42, no. 4, pp. 1386-1395, Oct. 2006.

R. E. Phelts and D. M. Akos

Nominal signal deformations: Limits on GPS range accuracy In Proc. Int. Symp. GNSS/GPS, 2004, vol. 6, paper. 8.

R. E. Phelts, J. Blanch, T. Walter, and P. Enge

The effect of nominal signal deformation biases on ARAIM

In Proc. Int. Tech. Meeting Inst. Navig., 2014, pp. 56-67.

Advanced RAIM user algorithm description: Integrity support message processing, fault detection, exclusion, and protection level calculation

In Proc. 25th Int. Tech. Meeting Satell. Division Inst. Navig., 2012, pp. 2828-2849.

J. Blanch et al. [7]

> Architectures for advanced RAIM: Offline and online In Proc. ION GNSS+ 2014, 2014, pp. 787-804.

- M. Joerger, F. C. Chan, and B. Pervan Solution separation versus residual-based RAIM Navigation, vol. 61, no. 4, pp. 273-291, 2014.

Integrated GPS/inertial fault detection availability Navigation, vol. 43, no. 2, pp. 111-130, Jun. 1996.

[10] B. S. Pervan, S. P. Pullen, and J. R. Christie

> A multiple hypothesis approach to satellite navigation integrity Navigation, vol. 45, no. 1, pp. 61-71, 1998.

[11] J. Blanch et al.

Baseline advanced RAIM user algorithm and possible improve-

IEEE Trans. Aerosp. Electron. Syst., vol. 51, no. 1, pp. 713-732, 2015.

J. Blanch, T. Walter, and P. Enge [12] Optimal positioning for advanced RAIM

Navig. J. Inst. Navig., vol. 60, no. 4, pp. 279-289, 2013.

Critical elements for a multi-constellation advanced RAIM Navigation, vol. 60, no. 1, pp. 53-69, 2013.

[14] Y. C. Lee

> New advanced RAIM with improved availability for detecting constellation-wide faults, using two independent constellations Navigation, vol. 60, no. 1, pp. 71-83, 2013.

Y. Zhai, M. Joerger, and B. Pervan [15]

> Continuity and availability in dual-frequency constellation ARAIM

In Proc. ION GNSS, 2015, pp. 664-674.

[16] M. A. Sturza

Navigation system integrity monitoring using redundant mea-

Navigation, vol. 35, no. 4, pp. 483-501, Dec. 1988.

[17] R. G. Brown

A baseline GPS RAIM scheme and a note on the equivalence of three RAIM methods

Navigation, vol. 39, no. 3, pp. 301-316, 1992.

- [18] B. W. Parkinson and P. Axelrad A basis for the development of operational algorithms for simplified GPS integrity checking *Inst. Navigation, Tech. Meeting*, 1987, vol. 1, pp. 269–276.
- [19] T. Walter and P. Enge Weighted RAIM for precision approach In *Proc. ION GPS*, 1995, pp. 1995–2004.
- [20] Y. C. Lee Analysis of range and position comparison methods as a means to provide gps integrity in the user receiver In *Proc. 42nd Annu. Meeting Inst. Navigation*, 1986, pp. 1–4.
- [21] M. Joerger and B. Pervan Fault detection and exclusion using solution separation and chisquared ARAIM *IEEE Trans. Aerosp. Electron. Syst.*, vol. 52, no. 2, pp. 726–742, Apr. 2016.
- [22] A. Ray and M. Desai A redundancy management procedure for fault detection and isolation ASME, Trans. J. Dyn. Syst. Meas. Control, vol. 108, pp. 248–254, 1986.

- [23] B. W. Parkinson and P. Axelrad Autonomous GPS integrity monitoring using the pseudorange residual Navigation, vol. 35, no. 2, pp. 255–274, 1988.
- [24] M. E. Peters, R. M. Gates, and M. Chertoff 2008 federal radionavigation plan In *Proc. Natl. Tech. Inf. Serv*, vol. 22161, 2009.
- [25] J. Speidel, M. Tossaint, S. Wallner, and J. Angelávila-Rodriguez Integrity for Aviation: Comparing Future Concept In *Proc. Insid. GNSS*, pp. 54–64, 2013.
- [26] C. Macabiau et al. Nominal bias analysis for ARAIM User In Proc. ION Int. Tech. Meeting, 2015, pp. 713–732.
- 27] I. E. Potter and M. C. Suman

 Threshold-less Redundancy Management With Arrays of Skewed Instruments

 AGARDOGRAPH No 224, 1977, pp. 15–11 to 15–25.